Interfaced Metal Heterodimers in the Quantum Size Regime

Journal:	*Nano Letters*
Manuscript ID:	nl-2013-02361b.R1
Manuscript Type:	Communication
Date Submitted by the Author:	19-Jul-2013
Complete List of Authors:	Gray, Stephen; Argonne National Laboratory, Center for Nanoscale Materials Sun, Yugang; Argonne National Laboratory, Center for Nanoscale Materials Foley, Jonathan; Argonne National Laboratory, Center for Nanoscale Materials Peng, Sheng; Argonne National Laboratory, Center for Nanoscale Materials Li, Zheng; University of Arkansas, Department of Chemistry and biochemistry

Interfaced Metal Heterodimers in the Quantum Size Regime

Yugang Sun,[†] Jonathan J. Foley,[†] Sheng Peng,[†] Zheng Li, and Stephen K. Gray[*]*

Center for Nanoscale Materials, Argonne National Laboratory, 9700 South Cass Avenue,
Argonne, Illinois 60439, United States

RECEIVED DATE (to be automatically inserted after your manuscript is accepted if required according to the journal that you are submitting your paper to)

ABSTRACT. Synthesis of nanoparticle dimers made of asymmetric compositions is very challenging because of the difficulty in manipulating the nanoparticles' surface chemistries in order to control the assembly and/or growth of different nanoparticles. In this Letter, we report a seed-mediated, surface-confined epitaxial overgrowth strategy that enables the synthesis of high-quality interfaced Au-Ag heterodimers in the quantum size regime (diameters <10 nm). Au and Ag share a common face-centered cubic lattice and have nearly identical lattice constants, which facilitates epitaxial overgrowth and allows direct contact between the Au and Ag domains. Quantum size effects, formation of the Au/Ag interfaces, and chemical interactions with surfactant molecules strongly influence the optical properties of the dimers and lead to the observation of unique surface plasmon resonances. In particular, we find an unusual enhancement of the characteristic Au surface plasmon resonance and the emergence of a charge transfer plasmon across the Au/Ag domains, which together lead to broad-band absorption spanning visible to near-infrared wavelengths. A model which captures the changes in optical behavior due to chemical interactions and quantum size effects is used to calculate the absorption spectra of the interfaced heterodimers, resulting in good agreement with experimental measurements.

KEYWORDS. Metal nanoparticle dimers, surface plasmon resonance, plasmomics, quantum-size effects, epitaxial overgrowth, discrete dipole approximation

Noble metal nanoparticles, typically gold (Au) and silver (Ag), have been extensively studied because of their unique optical properties associated with surface plasmon resonances (SPRs), leading to the establishment of the field of "plasmonics".[1] The SPRs of nanoparticles in the small particle limit can significantly deviate from SPRs of larger nanoparticles due to quantum size effects. For example, Scholl, Koh and Dionne used monochromated scanning transmission electron microscopy (STEM) electron energy-loss spectroscopy (EELS) to study SPRs of individual ligand-free Ag nanoparticles with diameters ranging from 20 nm to less than 2 nm and identified a transition into a quantum regime characterized by a substantial blueshift in the resonance position with decreasing particle size.[2] Another example is from our own work wherein we synthesized highly uniform colloidal Ag nanoparticles with varying diameters in the range of 2-20 nm. The SPR peak position of these colloidal Ag nanoparticles exhibited exceptional size dependence, i.e., initially blue-shifting as size decreased from ~20 nm but then strongly red-shifting with decreasing size from ~12 nm down to 2 nm.[3] Theoretical modeling suggested that surfactant-Ag interactions lowered the electron conductivity of the outermost Ag layers of the nanoparticles and strongly influenced the positions of the SPR peaks. This effect could be termed a "quantum chemical" size effect. Size effects, of course, are not limited to isolated monomer systems. In nanoparticle dimer systems, the separation gap between the monomer units also provides an additional source of quantum size effects. Recent experimental and theoretical studies have demonstrated deviations from classical theories occurring for small gaps (<1 nm) and correlated these results with quantum tunneling.[4–10]

In spite of advances such as those outlined above, preparing samples that allow comprehensive study of quantum effects and the role of chemical interactions remains fundamentally challenging, particularly when the constituent nanoparticles are small. For instance, in the study of ref. 6, precise measurement of small Ag nanoparticle pairs in the regimes between 0.5 nm gap and touching was not possible under electron beam illumination because the sudden merging of the nanoparticles lead to a dramatic change in morphology, which in itself has a significant influence on the SPR properties. In addition, it is extremely difficult to form a nanoparticle pair consisting of two nanoparticles made of different materials (for example, Ag and Au) through the random assembly of nanoparticles on a TEM grid. Although assembly of individual Au and Ag nanoparticles with sizes of tens of nanometers into Au-Ag heterodimers was demonstrated by using specific linker molecules,[11] the formation of Au-Ag heterodimers in the small-particle limit has not been realized and thus their potential useful properties remain relatively unexplored. Most recently, Liang et al. reported the direct growth of symmetric or asymmetric Ag domains on anisotropic Au nanorods coated with hexadecyltrimethylammonium bromide (CTAB) by controlling pH value of the reaction solution.[12] The as-grown Ag domains were able to be converted to semiconductor components, such as Ag2Se and CdSe.

Herein we report, for the first time, the synthesis of high-quality interfaced Au-Ag heterodimers in the quantum size regime (diameters <10 nm) with the use of isotropic spherical Au nanoparticles as the starting materials. Each heterodimer consists of a spherical Au nanoparticle and a Ag nanoparticle epitaxially grown from the Au nanoparticle. The Au-Ag heterodimers are synthesized in high yield and the size of the Ag nanodomains can be controlled by reaction time. Growth of the interfaced Ag nanodomains brings about several remarkable optical features, including an unexpected enhancement of gold's SPR and the emergence of a broad, charge transfer plasmon (CTP), which is characterized by charge oscillations between the Au and Ag domains.[7,8,10,13,14] When the Ag domains are comparable or larger in size than the Au spheres, these resonances contribute to broad-band absorption spanning visible to near-infrared wavelengths. The precise tunability of the structural features makes these particles especially suitable for performing comprehensive experimental and theoretical studies of the relationship between structure and the unique optical properties that arise from chemical interactions and quantum size effects, which in turn will provide valuable insight into how plasmonic materials can be engineered for catalytic, sensing, and other purposes in the small-particle limit.

The synthesis of interfaced Au-Ag heterodimers starts with the preparation of highly uniform Au nanoparticles through reduction of $HAuCl_4$ with *tert*-butylamine-borane complex (TBAB) in a mixed solvent of oleylamine (OAm)/1,2,3,4-tetrahydronaphthalene (tertalin) at room temperature.[15] The synthesized Au particles are highly monodisperse and exhibit an average diameter of 5.9 nm (Figure S1A). The Au nanoparticles can be used as seeds to mediate the deposition of a conformal layer of amorphous iron oxide on the nanoparticles through the decomposition of $[Fe(CO)_5]$ in hot 1-octadecene (ODE) containing a small amount of OAm as surfactant.[16,17] The iron oxide layer can prevent the surfaces of the Au nanoparticles from reacting with other species. When the iron oxide layer is very thin and only passivates partial surfaces of the Au nanoparticles, the Au surfaces that are not covered with iron oxide can provide the active surfaces to drive an epitaxial overgrowth of Ag, leading to the formation of interfaced heterodimers with direct contacts between the Ag domains and the Au nanoparticles. Figure 1A presents a typical TEM image of the Au nanoparticles after they have been exposed to the decomposition of $[Fe(CO)_5]$ for a very short time. The energy-dispersive X-ray spectra (EDS) of these nanoparticles exhibit strong Fe signals (Figure S1D) that are not observed from the as-synthesized Au nanoparticles (Figure S1). In addition, the inter-particle distance in the self-assembled arrays of the iron oxide coated Au nanoparticles is larger than that of Au nanoparticles without iron oxide coating (Figure S1C versus Figure S1A). These comparisons clearly indicate the existence of iron oxide coating after the Au nanoparticles have been exposed to [$Fe(CO)_5$]. The Au nanoparticles barely coated with iron oxide can serve as seeds to promote the condensation and growth of interfaced Ag domains on their surfaces when the Au nanoparticles are mixed with $AgNO_3$ in hot OAm/ODE. Reduction of $AgNO_3$ by OAm results in the formation of peanut-shaped Au-Ag dimers with tunable Ag nanodomains depending on the reaction time. The as-synthesized dimers are then washed with hexane and re-dispersed in hexane for characterization. As shown in Figures 1B-F, the size of the Ag domains monotonically increases as the reaction proceeds.

High-resolution TEM (HRTEM) images (Figures 1G-I) of the dimers reveal that the crystalline lattice of the Ag domains are in direct contact with that of the Au nanoparticles, indicating that condensation of Ag atoms on the surface of Au is easier than on the surface of iron oxide. The crystalline lattices in the Ag and Au domains exhibit an epitaxial relationship that lowers the energy barrier for growing Ag nanodomains on the Au surface rather than on the iron oxide.[18] The epitaxial overgrowth of Ag on the Au surface is ascribed to the close match between the lattice constants of Ag and Au (i.e., 4.090 Å for Ag *vs.* 4.080 Å for Au). Due to the formation of epitaxial interfaces between the Ag and Au nanodomains, the synthesized particles shown in Figure 1 are referred to as "interfaced Au-Ag heterodimers". Careful analysis of TEM images and EDS spectra after various reaction times allows us to correlate the geometrical parameters of the simple model heterodimer structure shown in Figure S2A with reaction time. This model corresponds to a Au sphere with the interfaced Ag nanodomain being the non-overlapping portion of another sphere that is displaced from the Au one (See the Supporting Information, Figure S2, for details). For example, the diameter of the Au spheres remains 5.9

nm while the maximum thickness of the crescent-shaped Ag nanodomains ranges from 2.0 nm at 2 s to 3.9 nm at 180 s.

Due to their high uniformity and purity, the interfaced Au-Ag heterodimers provide an ideal class of materials for studying the effects of surface chemical interactions (including both organic surfactant and interfaced metal) and quantum size effects on SPRs. The SPRs of the interfaced Au-Ag heterodimers are examined by measuring absorption spectra of the heterodimers dispersed in hexane. As shown in Figure 2, the Au nanoparticle seeds (i.e., at reaction time of 0 s) exhibit a broad asymmetric absorption peak at 548 nm with a full-width at half-max (FWHM) of ~70 nm. Mie theory calculations for a spherical Au nanoparticle with a diameter of 5.9 nm immersed in hexane (dielectric constant 1.88) yields a peak more than twice as narrow (FWHM ~30 nm) and centered on 525 nm (not shown) when the dielectric function of the bulk gold is used.[19] The broadness of the experimentally observed peak and it's ~20 nm red shift relative to the simple Mie theory result is ascribed to the surface damping associated with small size of the Au nanoparticles and chemical interactions with surfactant molecules.[3] Most interestingly, the peak intensity of the Au nanoparticles is significantly enhanced by about 50%, and the peak-width is slightly narrowed upon formation of the Au-Ag interface at reaction time of 2 s (red curve, Figure 2). Because the Au nanoparticles are not changed during the deposition of the Ag domains, the changes of the absorption peak originate from the formation of the Au/Ag interface. The absorption spectrum of the interfaced Au-Ag heterodimers formed at 2 s does not show the characteristic Ag SPR band (expected to be near 410 nm), indicating that the formation of Au/Ag interface may damp the SPR in the Ag domains. Figure 2 further shows that as the Ag domains become larger (reaction times increase beyond 2 s), the absorption peak around the Au SPR position shifts to the red and a new absorption peak gradually develops around the characteristic Ag SPR position. A third SPR peak emerges near 600 nm at the reaction time of 90 s when the size of the Ag domains is similar to that of the Au nanoparticles. The absorption spectrum of the interfaced Au-Ag heterodimers, when the Au and Ag nanodomains are of comparable size, exhibit three well-defined peaks: i) one at ~410 nm close to the Ag SPR position, ii) one at ~540 nm close to the Au SPR position, iii) one at longer wavelength (>600 nm). In the remainder of the text, these absorption peaks are referred to as PK1, PK2, and PK3, respectively, for simplicity. As the Ag domains continue to grow, PK2 slightly blue shifts while PK3 significantly red shifts. Both the peaks gain intensity and eventually span overlapping spectral regions between 500 and 900 nm.

When the reaction time is long enough (≥7 min), the intensity of PK1 becomes essentially constant (Figure S3), indicating that the growth of the Ag domains stops due to the complete consumption of $AgNO_3$. The size of the Ag domains in the resulting interfaced Au-Ag heterodimers is approximately three times that of the Au nanoparticles. HRTEM images of the individual dimers also clearly show the epitaxial relationship at the Au/Ag interfaces (Figure S4). It is worth noting that the intensities of both PK2 and PK3 at 7 min are lower than those at 4 min and continue to decrease with increasing reaction time beyond 4 minutes (Figure S3). TEM images of the products show that the Ag nanodomains eventually detach from the Au following incubation at high temperature (180 °C) for long times (Figure S5). The separation between the Au and Ag nanoparticles is ascribed to the decreased interfacial compressive stress from the Ag nanodomains with increasing size.[20] The detachment at long reaction times indicates that alloying between Au and Ag in the interfaced Au-Ag heterodimers is negligible.

Due to the small size of the particles and the large surface-to-volume ratio, we expect that quantum size effects and chemical interactions with surfactant molecules will contribute significantly to the observed SPR behavior. Indeed, classical electrodynamics calculations using the discrete dipole approximation (DDA)[21,22] and the bulk dielectric constant data of Johnson and Christy for Ag and Au[19] for the heterodimers immersed in hexane lead to absorption spectra, Figure 3A, that differ from the experimental results in several key aspects. Unless otherwise stated, our DDA-based cross sections are all the result of orientational averages so that they may be directly compared with the experimental results (see Supporting Information). Relative to the experimental results of Figure 2, the calculated peaks in Figure 3A are both significantly narrower; PK1 at 180 s is calculated to have a FWHM of 25 nm compared to the experimentally measured FWHM of ~50 nm and PK2 at 0 s is calculated to have a FWHM of ~30 nm compared to the experimentally measured FWHM of ~70 nm. Additionally, all three peaks are blue-shifted by 20-30 nm in the calculated spectra when bulk properties are assumed. Furthermore, the peak associated with the Au SPR near 525 nm in Figure 3A does not increase in magnitude as the size of the Ag nanodomain (or reaction time) increases.

While small, the synthesized nanoparticles are still too large to allow for reliable, fully quantum mechanical calculations of their optical properties. Nonetheless we can account for quantum size effects and chemical interactions in a phenomenological manner by size-correcting the dielectric constant of each of the metals in the heterodimer. DDA calculations, employing these size-corrected dielectric constants, are then used to obtain absorption spectra and other quantities of interest. The DDA calculations require, for each frequency or wavelength of considered, specification of the dielectric constant at each point in space. For points in space that are within a given metal of the heterodimer: (i) the intraband contribution to the metal's dielectric constant is modified to reflect damping of the conduction electrons[3, 23–27] and (ii) for points within the outer 0.25 nm layer of the heterodimer, following ref. 3, the intraband size correction also includes a reduction in conductivity in this outer layer owing to chemical interactions with the OAm surfactant. As with the calculations that lead to Figure 3A, we assume that the heterodimer is immersed in hexane. In order to correspond closely to the synthesized colloidal particles, we also assume that just outside the heterodimer there is a 2-nm shell of OAm surfactant (with a dielectric constant of 2.10), although this latter feature leads to very small spectral shifts relative to its exclusion.

Correction (i) mentioned in the preceding paragraph accounts for enhanced electron damping due to particle sizes becoming less than the classical mean free path of the conduction electrons. In applying it we use a generalization of the usual size correction suggested by Liu and Guyot-Sionnest for metals that are interfaced with one another.[26] This correction accounts for the importance of electron scattering and other damping effects at the various interfaces between materials X and Y with parameters $A_{X,Y}$. The dielectric constant in a region occupied by Au involves a contribution from electrons scattering at the Au-surfactant interface, $A_{Au,s}$, as well as a contribution from electrons scattering from the Au side of the Au/Ag interface, $A_{Au,Ag}$. Similarly, the dielectric constant in a region occupied by Ag involves parameters $A_{Ag,s}$ and $A_{Ag,Au}$ reflecting electrons in Ag scattering at the Ag-surfactant and Ag/Au interfaces. It turns out that $A_{Au,s}$, $A_{Ag,s}$, as well as the conductivity parameters involved in correction (ii) can all be fixed by requiring that the calculated spectra for only Au present (t = 0 s) and for when the Ag domain is dominant (t = 180 s) in accord with experiment. As a result, only the two metal interface parameters, $A_{Au,Ag}$ and $A_{Ag,Au}$, are to be determined such that the calculated spectra can describe the experimentally measured spectra as the Ag nanodomain increases. Consistent with general expectations, all the $A_{X,Y}$ parameters are found to be on the order of 1 or less and $A_{Ag,Au} > A_{Au,Ag}$. The difference between $A_{Ag,Au}$ and $A_{Au,Ag}$ reflects the increased tendency of electrons on the Ag side to interact with the metal-metal interface, which is consistent with the elementary expectations (i.e., Au is more electronegative than Ag) and the electronic structure calculations presented in Figure S6. Further discussion of all the model parameters and their specific values can be found in the Supporting Information.

With the theoretical model discussed above, the calculated spectra (Figure 3B) are in good agreement with experimentally measured SPR absorption spectra (Figure 2). In particular, results using this model show the unusual enhancement of PK2 and the emergence of the broad PK3 as increasing the size of the Ag domain. The modification of the electron density of the outermost metal layers accounting for the chemical interactions with the surfactant layer (correction (ii)) leads to the appropriate redshifts of the SPR peaks. Introducing quantum size effects (correction (i)) both broadens and helps to correct the relative intensities of the SPR absorption peaks. Using this model, PK1 at 180 s has a FWHM of ~50 nm in agreement with the experimental line width, while PK2 at 0 s has a FWHM of ~60 nm and is within 10 nm of the experimental line width. At 180 s, PK2 and PK3 are ~40% as intense as PK1 in the experimental spectrum. The calculated spectra with corrections (i) and (ii) find PK2 and PK3 to be ~30% as intense as PK1 at 180 s, whereas without correction, PK2 and PK3 are ~20% as intense as PK1.

For the larger Ag nanodomains, the model also allows us to attribute PK3 to a charge transfer plasmon (CTP). The conditions for a CTP require conductive overlap of different metal domains, and the intensity of the CTP is larger when there is close matching of the static conductivity of the domains, i.e., when $\frac{\sigma_{Au,0}}{\sigma_{Ag,0}} \cong 1$, where the static conductivity is given by $\sigma_{X,0} = \frac{\omega_X^2}{4\pi\gamma_X}$.[5] This ratio for the static conductivity of Au and Ag is ~0.32 when bulk values of γ_X and ω_X are used compared to ~1.23 in the size-corrected model. Hence, quantum size effects and chemical interactions in this case create a stronger condition for CTP resonances in the interfaced heterodimers and the synergy of these effects gives rise to broadband absorption.

Calculations with a fixed orientation along the inter-particle axis (i.e., longitudinal axis) of the interfaced Au-Ag heterodimers result in an absorption spectrum with two intense peaks at positions close to PK1 and PK3 (Figure 4A). Both longitudinal absorption peaks are broad and the absorption cross section, even at the peak valley position (~480-500 nm), is much larger than the absorption cross-section of the corresponding pure Au nanoparticle. The positions of both longitudinal peaks red shift and their intensities increase as the Ag domain increases in size. The calculated near-field electric field distribution shows that the longitudinal peak at the shorter wavelength essentially originates from the SPR of the Ag domain (top frame, Figure 4B). The peak at the longer wavelength is ascribed to the CTP where charge oscillates between the Au and Ag domains, which should have only a longitudinal contribution (Figure 4B).[5,7,8,10,13,14] Calculations along the transverse axis (i.e., the orientation perpendicular to the inter-particle axis) of the interfaced Au-Ag heterodimers lead to the observation of two absorption peaks at positions that are consistent with the characteristic SPR peaks of Au and Ag nanospheres (Figure 4C). As the size of the Ag domain increases the absorption cross section at the position of the Ag SPR increases accordingly while the absorption cross section at the position of the Au SPR diminishes slightly and slightly blue shifts. Although the formation of Au/Ag interface in an Au-Ag heterodimer does not significantly influence the transverse absorption cross section at wavelengths >500 nm, there is evidence that for larger silver particle sizes, PK2 results from transverse surface charge oscillations on both Au and the Ag surfaces (Figure 4D). The comparable near field intensity on the surfaces of both Au and Ag domains in the interfaced Au-Ag heterodimer at wavelengths >500 nm indicates a cooperative behavior of electrons in Ag and

Au, with PK3 showing CTP character. As a result, contributions of SPRs in both Au and Ag account for the broad absorption peaks (PK2 and PK3) of the interfaced Au-Ag heterodimers, while PK1 originates mainly from the Ag domains including both longitudinal and transverse SPR components with comparable contributions. The PK2 also includes both longitudinal and transverse SPR components and the increase in intensity of PK2 along with the growth of the Ag domains mainly originates from the longitudinal SPR component. The PK3 is dominated by the longitudinal SPR component.

In summary, interfaced Au-Ag heterodimers in the quantum size regime with tunable domain sizes have been successfully synthesized through the asymmetrically epitaxial overgrowth of Ag on partially passivated Au nanoparticles. The heterodimers support remarkable SPR modes including an unusually intense mode in the spectral region of the characteristic Au SPR and a broad mode that extends into near-infrared wavelengths. This behavior results from the synergistic interplay of the chemical interactions between the metal domains and the surfactant and quantum size effects. Calculations reveal that the SPRs in either Au or Ag domains exhibit broadband (400-900 nm) absorption, making them a possible class of photocatalysts with efficient ultilization of visible light and high surface area associated with their small sizes.[28,29]

ASSOCIATED CONTENT

Supporting Information

Details of the synthesis of interfaced Au-Ag heterodimers, details of theory and modeling for DDA calculations, details for the first principles calculations of $Ag_{14}Au_{10}$ clusters, Figures S1-6. This material is available free of charge via the internet at http://pubs.acs.org.

AUTHOR INFORMATION

Corresponding Author

*E-mail: (Y.S.) ygsun@anl.gov and (S.K.G.) gray@anl.gov

Author Contributions

Y.S., J.J.F., S.P. contributed equally. Y.S. and S.P. conceived the experiments. Y.S., S.P. and Z.L. performed the experiments. J.J.F. and S.K.G. carried out the calculations. All authors analyzed the data and wrote the manuscript.

Notes

The authors declare no competing financial interests.

ACKNOWLEDGMENTS

This work was performed at the Center for Nanoscale Materials, a U.S. Department of Energy, Office of Science, Office of Basic Energy Sciences User Facility under Contract No. DE-AC02-06CH11357. The electron microscopy was partially accomplished at the Electron Microscopy Center at Argonne National Laboratory, a U.S. Department of Energy Office of Science Laboratory under contract No. DE-AC02-06CH11357 by UChicago Argonne, LLC. Help from Dr. Yuzi Liu on electron microscopy is appreciated. JJF gratefully acknowledges Dr. Piotr Flatau for helpful discussion regarding convergence of the DDA method.

REFERENCES

1. Halas, N. J. *Nano Lett.* **2010,** *10*, 3816-3822.
2. Scholl, J. A.; Koh, A. L.; Dionne, J. A. *Nature* **2012,** *483*, 421-427.
3. Peng, S.; McMahon, J. M.; Schatz, G. C.; Gray, S. K.; Sun, Y. *Proceedings of the National Academy of Sciences* **2010,** *107*, 14530-14534.
4. Savage, K. J.; Hawkeye, M. M.; Esteban, R.; Borisov, A. G.; Aizpurua, J.; Baumberg, J. J. *Nature* **2012,** *491*, 574-577.
5. Esteban, R.; Borisov, A. G.; Nordlander, P.; Aizpurua, J. *Nat. Commun.* **2012,** *3*, 825.
6. Scholl, J. A.; García-Etxarri, A.; Koh, A. L.; Dionne, J. A. *Nano Lett.* **2013,** *13*, 564-569.
7. Pérez-González, O.; Zabala, N.; Aizpurua, J. *New J. Phys.* **2011,** *13*, 083013.
8. Zuloaga, J.; Prodan, E.; Nordlander, P. *Nano Lett.* **2009,** *9*, 887-891.
9. Atay, T.; Song, J.-H.; Nurmikko, A. V. *Nano Lett.* **2004,** *4*, 1627-1631.
10. Song, P.; Nordlander, P.; Gao, S. *J. Chem. Phys.* **2011,** *134*, 074701.
11. (a) Sheikholeslami, S.; Jun, Y.-w.; Jain, P. K.; Alivisatos, A. P. *Nano Lett.* **2010,** *10*, 2655-2660. (b) Hu, Y.; Sun, Y. *J. Am. Chem. Soc.* **2013,** *135*, 2213-2221.
12. Liang, S.; Liu, X.-L.; Yang, Y.-Z.; Wang, Y.-L.; Wang, J.-H.; Yang, Z.-J.; Wang, L.-B.; Jia, S.-F.; Yu, X.-F.; Zhou, L.; Wang, J. B.; Zeng, J.; Wang, Q.-Q.; Zhang, Z. *Nano Lett.* **2012**, *12*, 5281-5286.
13. Lassiter, J. B.; Aizpurua, J.; Hernandez, L. I.; Brandl, D. W.; Romero, I.; Lal, S.; Hafner, J. H.; Nordlander, P.; Halas, N. J. *Nano Lett.* **2008,** *8*, 1212-1218.
14. Zhao, K.; Troparevsky, M. C.; Xiao, D.; Eguiluz, A. G.; Zhang, Z. *Phys. Rev. Lett.* **2009,** *102*, 186804.
15. Peng, S.; Lee, Y.; Wang, C.; Yin, H.; Dai, S.; Sun, S. *Nano Res.* **2008,** *1*, 229-234.
16. Peng, S.; Lei, C.; Ren, Y.; Cook, R. E.; Sun, Y. *Angew. Chem. Int. Ed.* **2011,** *50*, 3158-3163.
17. Sun, Y. *Chem. Soc. Rev.* **2013,** *42*, 2497-2511.
18. Sun, Y.; Wiley, B.; Li, Z.-Y.; Xia, Y. *J. Am. Chem. Soc.* **2004,** *126*, 9399-9406.
19. Johnson, P. B.; Christy, R. W. *Phys. Rev. B* **1972,** *6*, 4370-4379.
20. Wang, C.; Wei, Y.; Jiang, H.; Sun, S. *Nano Lett.* **2009,** *9*, 4544-4547.
21. Draine, B. T.; Flatau, P. J. *J. Opt. Soc. Am. A* **1994,** *11*, 1491-1499.
22. Flatau, P. J.; Draine, B. T. *Opt. Exp.* **2012,** *20*, 1247-1252.

23. Genzel, L.; Martin, T. P.; Kreibig, U. *Z. Physik. B* **1975,** *21*, 339-346.

24. Kraus, W. A.; Schatz, G. C. *J. Chem. Phys.* **1983,** *79*, 6130-6139.

25. Coronado, E. A.; Schatz, G. C. *J. Chem. Phys.* **2003,** *119*, 3926-3924.

26. Liu, M.; Guyot-Sionnest, P. *J. Phys. Chem. B* **2004,** *108*, 5882-5888.

27. Sun, Y.; Gray, S. K.; Peng, S. *Phys. Chem. Chem. Phys.* **2011,** *13*, 11814-11826.

28. Christopher, P.; Xin, H.; Linic, S. *Nat. Chem.* **2011,** *3*, 467-472.

29. Linic, S.; Christopher, P.; Ingram, D. B. *Nat. Mater.* **2011,** *10*, 911-921.

Figure Captions

Figure 1. TEM images of the Au nanoparticles with surfaces partially passviated with iron oxide (A) before and (B-F) after the epitaxial overgrowth of Ag domains on their surfaces for different times: (B) 10 s, (C) 20 s, (D) 60 s, (E) 120 s, and (F) 180 s. (G-I) Representative HRTEM images of individual interfaced Au-Ag heterodimers formed at (G) 60 s, (H) 120 s, and (I) 180 s. The inter-planar distance measured from the adjacent lattice fringes in (G-I) is 0.236 nm, matching well with the (111) crystalline planes of face-centered cubic Au and Ag. The scale bar in (F) applies for (A-F) and the scale bar in (I) applies for (G-I). Specific domain size information at the various times can be found in the Supplementary Information in Figure S2.

Figure 2. Absorption spectra of the partially passivated Au nanoparticles shown in Figure 1A (0 s) and the corresponding interfaced Au-Ag heterodimers formed after the growth of the Ag domains for different times (labeled in legend). The nanoparticles were dispersed in hexane for spectral characterization. The intensities of the spectra were normalized against the concentration of the Au nanoparticles that was maintained constant during the synthesis.

Figure 3. Theoretically calculated absorption spectra of the interfaced Au-Ag heterodimers with different sizes of the Ag domains. The sizes of the Ag domains at different reaction times were determined by the EDX compositional analysis and the TEM images and summarized in Figure S2. In the spectra shown in (A), bulk dielectric properties of Ag and Au were assumed and the effects of the surfactant layer were ignored. In the spectra shown in (B), damping contributions from unique interfaces and quantum size effects were considered through Eq. (S6) and the

effects of the surfactant layer were also considered. Specific domain size information at the various times can be found in the Supplementary Information in Figure S2.

Figure 4. Single-orientation absorption cross sections calculated using the dielectric functions corrected for chemical interactions with the surfactant layer and quantum size effects. (A, C) Absorption cross sections of the interfaced Au-Ag heterodimers with differently sized Ag domains as the response to (A) the incident light polarized parallel to the inter-particle axes (i.e., longitudinal axes) of the dimers and (C) the incident light perpendicular to the inter-particle axes (i.e., transverse axes). (B, D) The simulated near-field electric field distribution for a dimer at 400 nm (top frames), 540 nm (middle frames), and 610 nm (bottom frames) (i.e., corresponding to the resonance wavelengths of PK1, PK2, and PK3) using the light polarized parallel (C) and perpendicular (D) to the inter-particle axis. The Ag domain in the heterodimer shown in (B, D) has a radius of 2.97 nm that is very close to that of the Au nanoparticle (2.95 nm). The diameter of the intersection circle and the overlap height between the Au and Ag domains are 4.60 nm and 2.19 nm, respectively. This dimer corresponds to the samples formed at the reaction time of 120 s (Figure 1E, Figure S2).

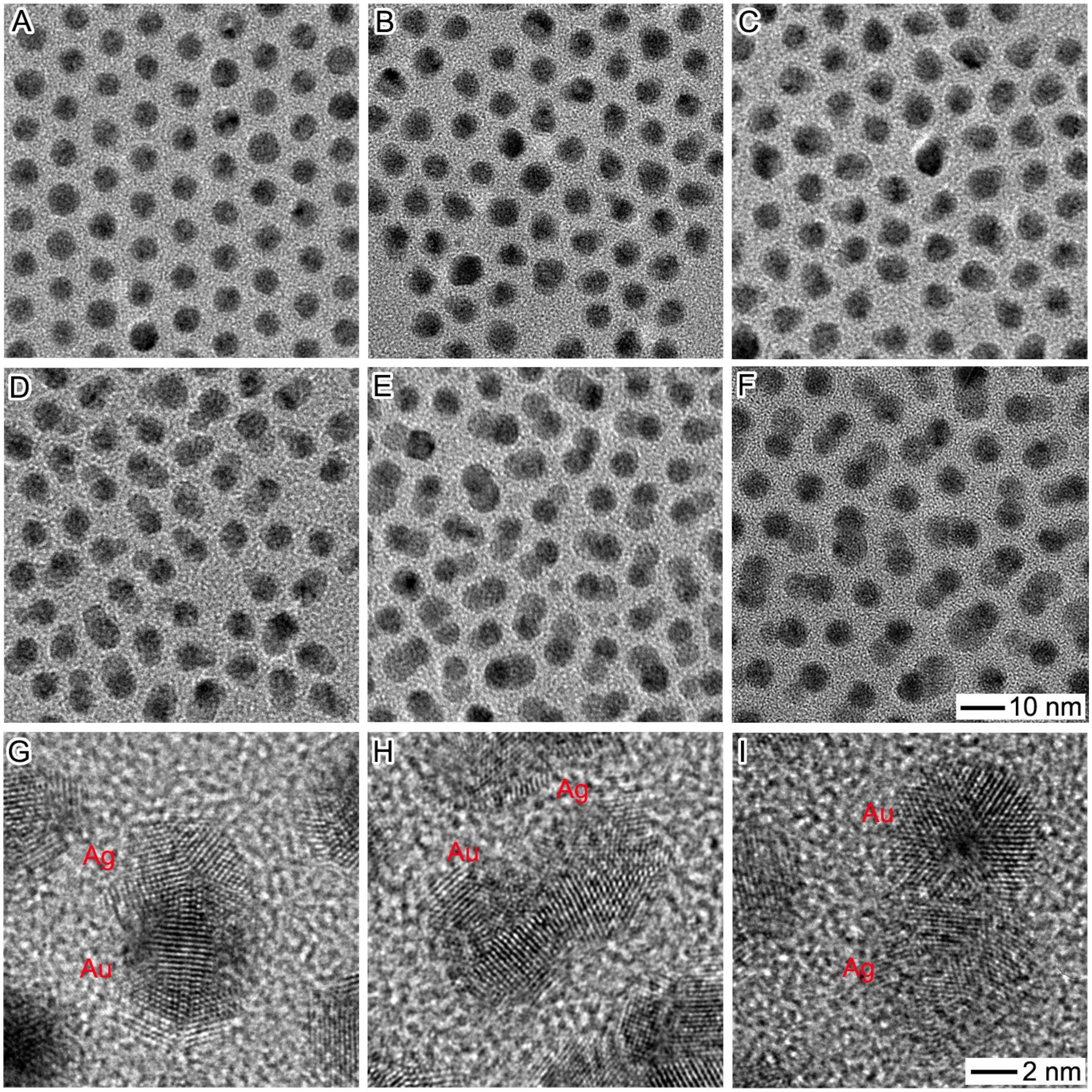

Figure 1

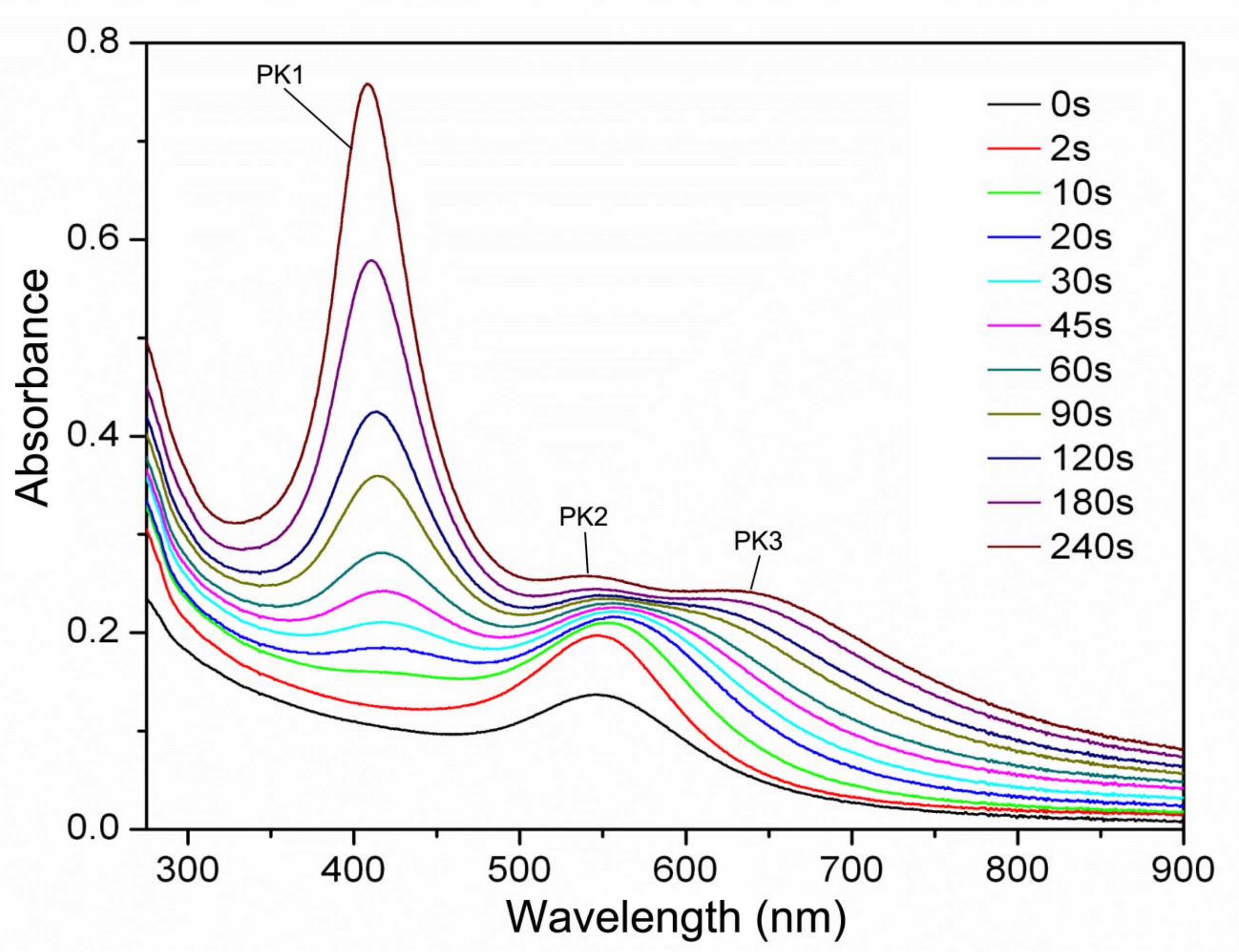
Absorbance
0.0
0.2
0.4
0.6
0.8
Wavelength (nm)
300
400
500
600
700
800
900
PK1
PK2
PK3
0s
2s
10s
20s
30s
45s
60s
90s
120s
180s
240s

Figure 2

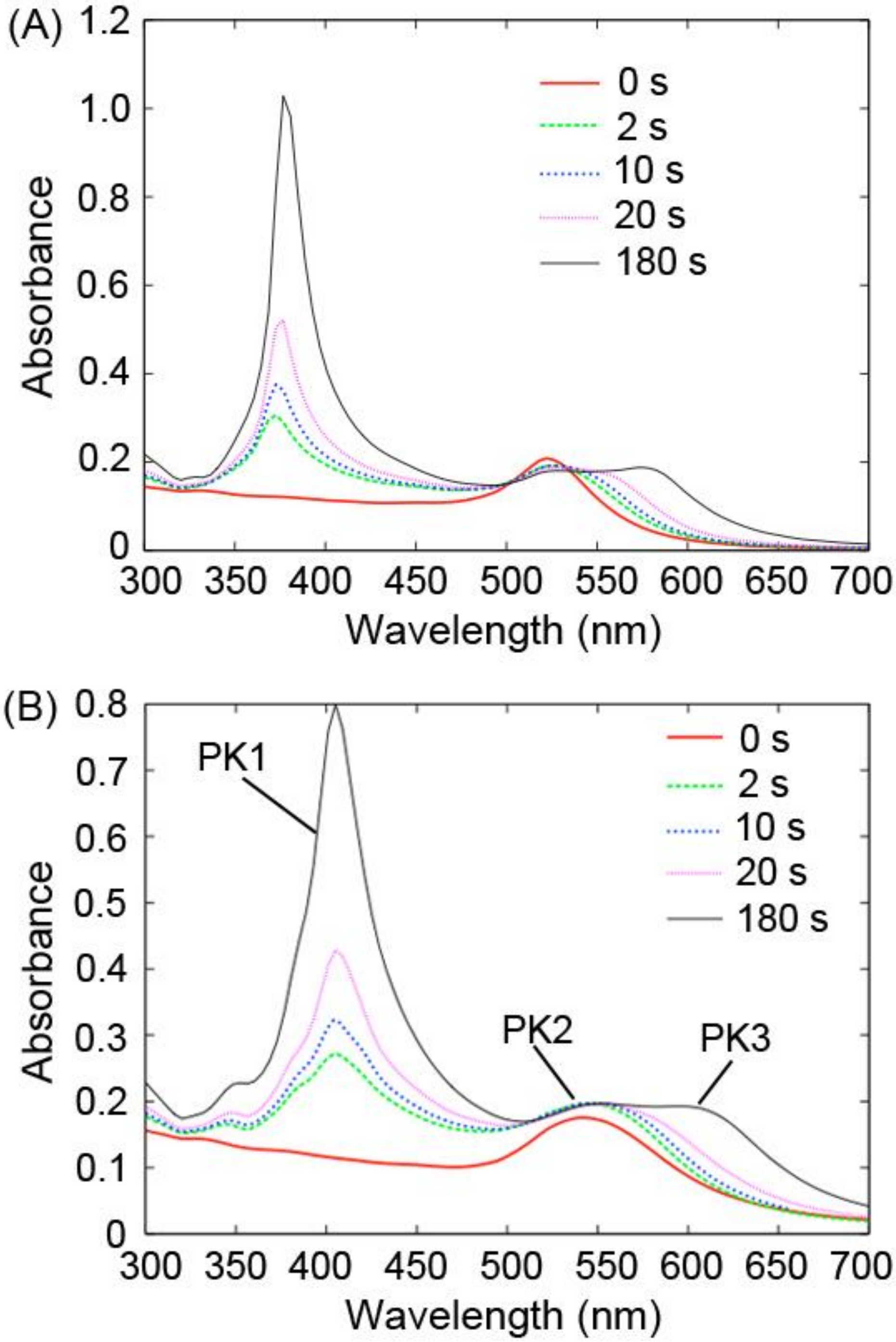
(A)
Absorbance
Wavelength (nm)
1.2
1.0
0.8
0.6
0.4
0.2
0
300
350
400
450
500
550
600
650
700
0 s
2 s
10 s
20 s
180 s
(B)
Absorbance
Wavelength (nm)
0.8
0.7
0.6
0.5
0.4
0.3
0.2
0.1
0
300
350
400
450
500
550
600
650
700
PK1
PK2
PK3
0 s
2 s
10 s
20 s
180 s

Figure 3

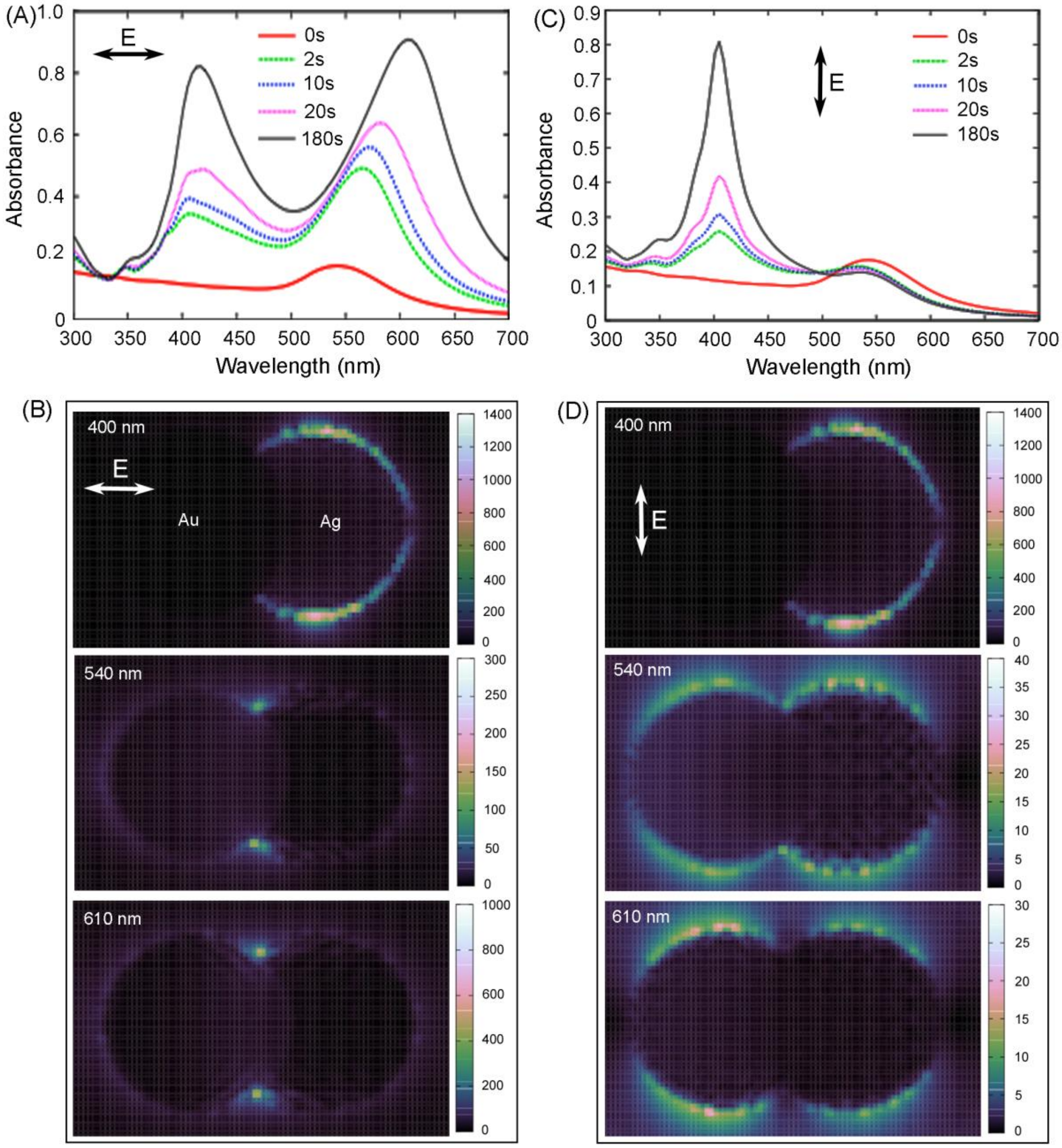
(A)
E
0s
2s
10s
20s
180s
Absorbance
Wavelength (nm)
0
0.2
0.4
0.6
0.8
1.0
300
350
400
450
500
550
600
650
700
(C)
E
0s
2s
10s
20s
180s
Absorbance
Wavelength (nm)
0
0.1
0.2
0.3
0.4
0.5
0.6
0.7
0.8
0.9
300
350
400
450
500
550
600
650
700
(B)
400 nm
E
Au
Ag
0
200
400
600
800
1000
1200
1400
540 nm
0
50
100
150
200
250
300
610 nm
0
200
400
600
800
1000
(D)
400 nm
E
0
200
400
600
800
1000
1200
1400
540 nm
0
5
10
15
20
25
30
35
40
610 nm
0
5
10
15
20
25
30

Figure 4

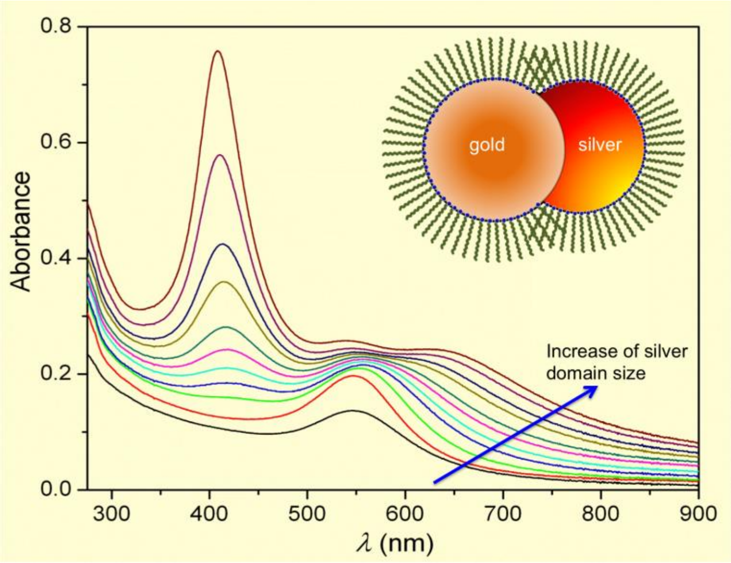

Artwork for TOC

sonance, plasmomics, quantum-

conductivity of the outermost Ag
s of the SPR peaks. This effect
ts, of course, are not limited to
the separation gap between the
ize effects. Recent experimental
sical theories occurring for small
g.[4–10]

preparing samples that allow
chemical interactions remains
t nanoparticles are small. For

high-quality interfaced Au-Ag
ith the use of isotropic spherical
ner consists of a spherical Au
e Au nanoparticle. The Au-Ag
g nanodomains can be controlled
brings about several remarkable
l's SPR and the emergence of a
y charge oscillations between the
rable or larger in size than the Au

s of the Au nanoparticles from
thin and only passivates partial
ot covered with iron oxide can
Ag, leading to the formation of
mains and the Au nanoparticles.
s after they have been exposed to
energy-dispersive X-ray spectra
S1D) that are not observed from
the inter-particle distance in the
icles is larger than that of Au

the Au surface rather than on the
ce is ascribed to the close match
vs. 4.080 Å for Au). Due to the
omains, the synthesized particles
mers”. Careful analysis of TEM
us to correlate the geometrical
Figure S2A with reaction time.
Ag nanodomain being the non-
the Au one (See the Supporting
er of the Au spheres remains 5.9

ith surfactant molecules.[3] Most
ficantly enhanced by about 50%,
Au-Ag interface at reaction time
ot changed during the deposition
from the formation of the Au/Ag
er dimers formed at 2 s does not
m), indicating that the formation
re 2 further shows that as the Ag
e absorption peak around the Au
gradually develops around the

he Au/Ag interfaces (Figure S4).
min are lower than those at 4 min
d 4 minutes (Figure S3). TEM
ly detach from the Au following
S5). The separation between the
compressive stress from the Ag
ng reaction times indicates that
ers is negligible.

-to volume ratio, we expect that
ctant molecules will contribute

arge to allow for reliable, fully
Nonetheless we can account for
ogical manner by size-correcting
r. DDA calculations, employing
ain absorption spectra and other
ch frequency or wavelength of
in space. For points in space that
and contribution to the metal's
ction electrons[3, 23–27] and (ii) for
owing ref. 3, the intraband size

f the Au/Ag interface, $A_{Au,Ag}$.
g involves parameters $A_{Ag,s}$ and
t and Ag/Au interfaces. It turns
olved in correction (ii) can all be
nt (t = 0 s) and for when the Ag
As a result, only the two metal
ch that the calculated spectra can
main increases. Consistent with
the order of 1 or less and $A_{Ag,Au}$
e increased tendency of electrons

tense as PK1 in the experimental

nd PK2 and PK3 to be ~30% as

K3 are ~20% as intense as PK1.

attribute PK3 to a charge transfer

tive overlap of different metal

is close matching of the static

static conductivity is given by

Ag is ~0.32 when bulk values of

d model. Hence, quantum size

ation of two absorption peaks at
f Au and Ag nanospheres (Figure
oss section at the position of the
on at the position of the Au SPR
tion of Au/Ag interface in an Au-
rst absorption cross section at
particle sizes, PK2 results from
Ag surfaces (Figure 4D). The
Ag domains in the interfaced Au-
e behavior of electrons in Ag and

either Au or Ag domains exhibit le class of photocatalysts with ted with their small sizes.[28,29]

tails of theory and modeling for $Ag_{14}Au_{10}$ clusters, Figures S1-6. pubs.acs.org.

y under Contract No. DE-AC02-
shed at the Electron Microscopy
t of Energy Office of Science
cago Argonne, LLC. Help from
atefully acknowledges Dr. Piotr
method.

.-Q.; Zhang, Z. *Nano Lett.* **2012**,

.; Romero, I.; Lal, S.; Hafner, J.

218.

Zhang, Z. *Phys. Rev. Lett.* **2009,**

Res. **2008,** *1*, 229-234.

em. Int. Ed. **2011,** *50*, 3158-3163.

04, *126*, 9399-9406.

379.

544-4547.

1-1499.

les were dispersed in hexane for were normalized against the nt during the synthesis.

rfaced Au-Ag heterodimers with s at different reaction times were mages and summarized in Figure g and Au were assumed and the wn in (B), damping contributions dered through Eq. (S6) and the particle (2.95 nm). The diameter

and Ag domains are 4.60 nm and

rmed at the reaction time of 120

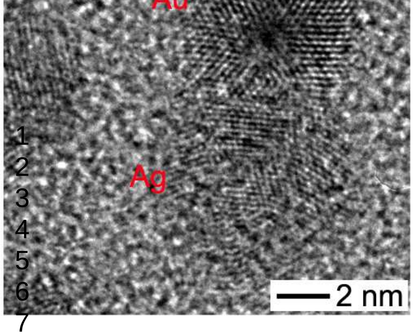
Au
Ag
2 nm

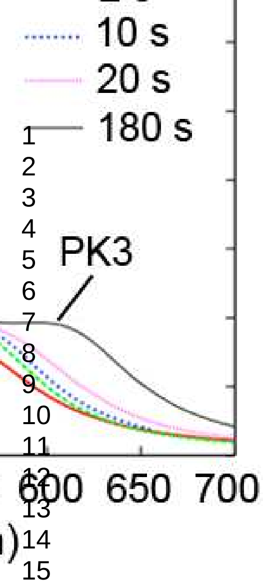
10 s
20 s
180 s
PK3
600
650
700

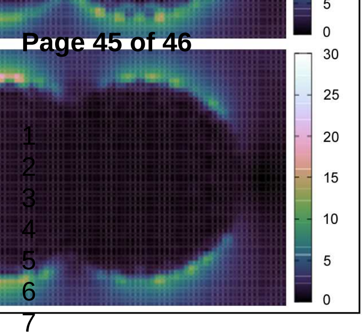
5
0
30
25
20
15
10
5
0